

DOI: 10.1002/celec.201402058

Buffer pK_a and Transport Govern the Concentration Overpotential in Electrochemical Oxygen Reduction at Neutral pH

Sudeep C. Popat,* Dongwon Ki, Michelle N. Young, Bruce E. Rittmann, and César I. Torres*^[a]

Microbial fuel cells (MFCs) show large cathodic overpotentials for the O_2 reduction reaction. The local cathode pH is important, as OH^- ions accumulate on the catalyst surface, resulting in a Nernstian concentration overpotential. Herein, we explore how various relevant buffers affect cathode performance at neutral pH, by reducing the concentration overpotential. We show that NH_4^+ buffer results in the best performance at current densities $> 10 A m^{-2}$, owing to buffering of the local pH close to its pK_a (ca. 9.2). With other buffers, the local pH in-

creases to > 12 at similar current densities. We also show the importance of diffusion in buffer transport. Increasing the buffer concentration or improving the hydrodynamic conditions leads to lower overpotentials. We also present a mathematical model that includes buffer diffusion, for use in predicting cathode polarization curves. Overall, our results point to the promise of reducing cathode overpotentials in MFCs using naturally available buffers.

1. Introduction


Because of the widespread availability of oxygen (O_2) and its relatively positive redox potential, the O_2 reduction reaction (ORR) is the cathodic reaction of choice in many fuel cells that aim to achieve combustionless electricity production from the anodic oxidation of fuels.^[1] In conventional chemical fuel cells, such as the proton exchange membrane (PEM) fuel cell or the alkaline fuel cell, ORR occurs under either acidic or basic conditions, respectively.^[2] However, recently emerging is a new class of fuel cells, referred to broadly as biological fuel cells (BFCs), in which the ORR needs to occur at near neutral pH, owing to the operational requirements of their biological components.^[3] These fuel cells include microbial fuel cells (MFCs), in which anodic oxidation of waste organics is carried out by anode-respiring bacteria that have the ability to transfer electrons resulting from metabolism directly to an anode, and enzymatic fuel cells, wherein enzymes are immobilized on electrodes to carry out catalyzed reactions.^[4] The latter also includes applications in which oxidase enzymes are immobilized on the cathode to catalyze the ORR;^[5] however, the study we present here applies directly only to BFCs that include a biological anode and a conventional metal-catalyst cathode.

From over a decade of research on BFCs, especially more so on MFCs, it has become apparent that power densities in these fuel cells are limited by a large cathodic overpotential, even if using precious metal catalysts such as platinum to cata-

lyze the ORR.^[6] Whereas large cathodic overpotentials have been recognized as a key issue in full-scale practical application of conventional chemical fuel cells, current densities achieved in MFCs at similar overpotentials are several orders of magnitude lower.^[7] This suggests a fundamental difference between the ORR at near neutral pH versus at acidic or basic pH. Thus, understanding the unique features of the ORR at near neutral pH and improving cathode performance are among the main challenges MFC researchers currently face in making them competitive against other technologies for energy recovery from organic waste streams.

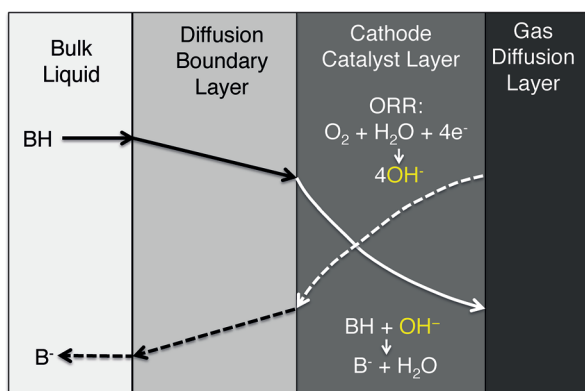
For MFCs that include a membrane between the anode and the cathode, poor cathode performance is attributed to the inevitable pH increase in the cathode chamber, often to > 12 .^[8] This results in a Nernstian concentration overpotential that is equivalent to approximately 60 mV for every unit the cathode pH is higher than the anode pH. One of the solutions proposed for this pH imbalance was to abandon the use of a membrane.^[9] Yet, single-chamber MFCs that lack a membrane still suffer from large cathodic overpotentials.^[10] We recently performed the first thorough study into understanding the origin of cathodic overpotentials in MFCs by considering closely the electrode–electrolyte interface.^[11] OH^- ions, which are a product of the ORR, accumulate locally on the surface of the cathode, because of their poor mass transport through the diffusion layer at the interface, as well as through the catalyst layer itself. This results in a Nernstian concentration overpotential owing to the localized accumulation of OH^- ions, irrespective of the use of a membrane. We showed that the local cathode pH could increase to up to a value of 13 at the typical current densities observed in MFCs upon using unbuffered electrolytes at neutral pH. This represents an overpotential of

[a] Dr. S. C. Popat, D. Ki, M. N. Young, Dr. B. E. Rittmann, Dr. C. I. Torres
Swette Center for Environmental Biotechnology
Biodesign Institute at Arizona State University
P.O. Box 875701, Tempe, AZ 85287-5701 (USA)
E-mail: scp@asu.edu
cit@asu.edu

 Supporting Information for this article is available on the WWW under <http://dx.doi.org/10.1002/celec.201402058>.

about 360 mV, or roughly 35% of the total voltage theoretically available (ca. 1.1 V) in MFCs.

In most MFCs, some form of buffer is added or is naturally present in the waste streams under consideration, and the buffer could possibly alleviate the problem of an increased pH on the cathode surface.^[12] In this study, we explore how different buffers affect the cathode performance through controlling the local cathode pH, focusing especially on two important parameters: the buffer pK_a and its effective diffusivity. We show in Scheme 1 how a buffer improves the performance of gas-



Scheme 1. A diagram of the electrode–electrolyte interface for air cathodes in MFCs. BH is the acidic buffer species, whereas B^- is the basic buffer species. The ORR occurs within the cathode catalyst layer, and the product of the reaction is OH^- , which is transported out by the buffer.

diffusion cathodes for ORR as they are used in single-chamber MFCs. The reaction produces OH^- , which deprotonates the acidic buffer species that transports from the bulk liquid to the active catalyst sites by diffusion and/or migration; this results in a lower local concentration of OH^- than having no buffer. The basic buffer species diffuses back to the electrolyte. This buffering mechanism should maintain the local cathode pH close to the pK_a of the buffer, as long as the rate of transport of the buffer species can match the rate of production of OH^- .

We present here a series of experiments, conducted with gas-diffusion half-cells containing platinum-based air cathodes for ORR that demonstrate how different relevant buffers contribute to improving cathode performance in MFCs. We also expand the mathematical model that we first presented in our previous study to include buffer speciation and transport. We also link our results to applications of MFCs in which high con-

centrations of certain buffers that are naturally present in some waste streams (e.g. NH_4^+) can be used to achieve improved energy recovery in MFCs.

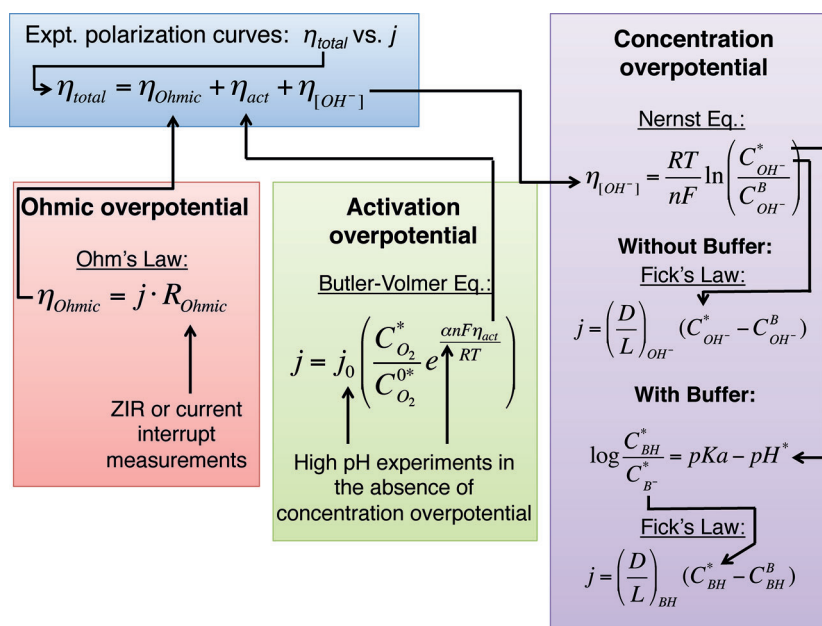
1.1. Overview of Cathode Modeling

We developed a mathematical model for the cathode to validate our results and quantify local cathode pH. This model follows that developed in our previous study,^[11] but includes buffer diffusion to the cathode and its speciation on the cathode catalyst. We describe below the details of the model, and how we used the model to determine 1) local pH on the cathode under a variety of conditions, and 2) the diffusion properties of OH^- and the buffers studied. We also show in Scheme 2 the model equations with a workflow of how we used them.

There are three primary overpotentials that affect the cathode polarization curves (η_{total} vs. j , in which η_{total} is the total experimental overpotential in V and j is the current density in $A\ m^{-2}$). These are the activation overpotential (η_{act}), the Ohmic overpotential (η_{Ohmic}), and the Nernstian concentration overpotential related to OH^- transport out of the cathode ($\eta_{[OH^-]}$). We assume that, for typical current densities achieved in air-cathode MFCs, concentration overpotential related to O_2 transport is at a minimum. This assumption is supported by the fact that we have never observed a limiting cathodic current density in our studies, nor have we found such an observation in the literature. Thus, the total overpotential can be represented by Equation (1):

$$\eta_{total} = \eta_{Ohmic} + \eta_{act} + \eta_{[OH^-]} \quad (1)$$

The Ohmic overpotential can be represented as shown in Equation (2) and can be determined through measuring the



Scheme 2. Model equations along with the workflow of how we used the model to determine the local cathode pH and D/L values for the various conditions tested.

Ohmic resistance (R_{Ohmic} ; Ohm cm^2) using either electrochemical impedance spectroscopy or the current interrupt method. All the polarization curves we show here are i - R corrected, that is, the Ohmic overpotential is subtracted from the total overpotential.

$$\eta_{\text{Ohmic}} = j \cdot R_{\text{Ohmic}} \quad (2)$$

Next, the activation overpotential can be represented as a function of the current density through the simplified version of the Butler–Volmer equation (assuming negligible reverse reaction kinetics). In Equation (3), j_0 , α , and n are the exchange current density in units of A m^{-2} , the charge-transfer coefficient, and the number of electrons transferred, respectively. $C_{\text{O}_2}^*$ and $C_{\text{O}_2}^{0*}$ represent the actual and standard concentrations of O_2 on the cathode, respectively, in units of mmol cm^{-3} . We assume that $n=4$ for the Pt/C electrodes we used in this study.

$$j = j_0 \left(\frac{C_{\text{O}_2}^*}{C_{\text{O}_2}^{0*}} e^{\frac{\alpha n F \eta_{\text{act}}}{RT}} \right) \quad (3)$$

As described in our previous study,^[11] we fit the Tafel equation, simplified from the Butler–Volmer equation, to polarization curves obtained in high pH, to determine the values of j_0 and α . In high pH, we assumed that the concentration overpotential is negligible, and thus the cathode performance is only governed by the activation overpotential. For the polarization curves we show here in neutral pH, we calculated the activation overpotential based on the Butler–Volmer equation and compared it against the total cathode overpotential observed experimentally. We assumed that the remainder of the overpotential is due to the Nernstian concentration overpotential, which can be defined by Equation (4):

$$\eta_{[\text{OH}^-]} = \frac{RT}{nF} \ln \left(\frac{C_{\text{OH}^-}^*}{C_{\text{OH}^-}^{\text{B}}} \right) \quad (4)$$

$C_{\text{OH}^-}^0$ and $C_{\text{OH}^-}^{\text{B}}$ are the local cathode and bulk liquid concentrations of OH^- ions, respectively, in units of mmol cm^{-3} . From this equation, we calculated the local cathode pH. Using the local cathode pH with Fick's Law allowed us to also determine the diffusion properties of OH^- and the buffer [Eq. (5)]:

$$J_x = \frac{D_x (C_x^* - C_x^{\text{B}})}{L} \quad (5)$$

J_x is the flux of solute x (either OH^- or acidic buffer species) in units of $\text{mmol cm}^{-2} \text{s}^{-1}$, D is its diffusion coefficient in units of $\text{cm}^2 \text{s}^{-1}$, and L is the diffusion length in cm. We do not differentiate between the diffusion boundary layer and the cathode catalyst layer. For the buffer, we determined the speciation of the acidic and basic components by its $\text{p}K_{\text{a}}$ using Equation (6):

$$\log \frac{C_{\text{B}}^*}{C_{\text{BH}}^*} = \text{p}K_{\text{a}} - \text{pH}^* \quad (6)$$

Combining speciation with diffusion allows us to determine an equilibrium pH at the cathode surface, and we compared that pH against the calculated value from the measured overpotential. The fitting parameter is D_x/L , which is associated with the transport of OH^- and acidic buffer species to the cathode surface. A separate value of D_x/L is used for both components of interest as we fit our experimental data, as the buffer governs the concentration overpotential in the range of pH around its $\text{p}K_{\text{a}}$, and OH^- governs the concentration overpotential at higher pH.

The model parameters we obtained are summarized in Table 1 for two different sets of experiments we performed: one with different buffer concentrations and the other with

Table 1. Modeling parameters for buffer concentration and stirring speed experiments.^[a]

	j_0 [A m^{-2}]	$D/L_{(\text{NH}_4^+)}$ [cm s^{-1}]	$D/L_{(\text{OH}^-)}$ [cm s^{-1}]
Buffer concentration experiments			
All buffer concentrations	2.1×10^{-4}	8.15×10^{-4}	6.59×10^{-4}
Stirring experiments [RPM]			
0	1.5×10^{-4}	6.52×10^{-4}	2.51×10^{-4}
30	1.5×10^{-4}	8.51×10^{-4}	2.64×10^{-4}
50	1.5×10^{-4}	8.58×10^{-4}	n.n. ^[b]
100	1.5×10^{-4}	9.32×10^{-4}	n.n.
300	1.5×10^{-4}	1.22×10^{-3}	n.n.
500	1.5×10^{-4}	1.22×10^{-3}	n.n.

[a] For all experiments, $\alpha = 0.209$ and $n = 4$. [b] n.n. = not needed.

different stirring rates inside the half cells. These parameters lie in the typical range for Pt/C cathodes.^[11] We performed all modeling using Excel 2010 Solver to minimize the difference between the observed and calculated flux from [Eq. (3)]. We attribute the small differences in j_0 upon fitting our data to minor differences in cathode preparation over multiple experiments and trials. These j_0 values correspond to an η_{act} of roughly 350 mV at a current density of 10 A m^{-2} , as can be seen in Figures 1 and 2.

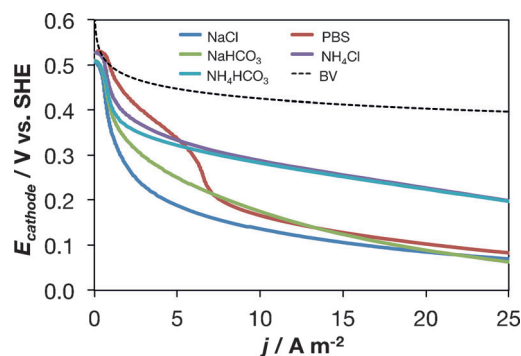


Figure 1. LSVs of a Pt-based gas-diffusion cathode in different solutions (50 mm each). The dotted line shows the Butler–Volmer curve on the basis of the j_0 and α values determined from high pH experiments.

2. Results and Discussion

We show in Figure 1 linear sweep voltammograms (LSVs) of cathodes in solutions (50 mM) of different buffers. As expected, even at low current densities, the cathode potential in the unbuffered NaCl solution (50 mM) decreased rapidly as a result of an increase in the local cathode pH, as we have shown before.^[11] Our previous analysis suggests that by 2 A m^{-2} , the local cathode pH already increases by five pH units in the absence of a buffer, thus representing a Nernstian concentration overpotential of about 300 mV owing to local accumulation of OH^- . At 10 A m^{-2} , the total overpotential is approximately 700 mV (considering an E^{0*} of $+0.81$ vs. SHE for ORR in pH 7). As η_{act} is roughly 350 mV, the remainder (50%) is $\eta_{[\text{OH}^-]}$.

In contrast, the cathode overpotential for current densities of up to 5 A m^{-2} was lower in phosphate buffer solution (PBS). This was a result of the buffering of pH whereupon H_2PO_4^- is deprotonated by OH^- ($\text{p}K_{\text{a}2}=7.2$). As shown below in detail for the case of NH_4^+ buffer, limitation owing to buffer transport is apparent from the inflection in the cathode potential, which for the phosphate buffer is observed after 5 A m^{-2} in the LSV. Bicarbonate buffer did not significantly help in maintaining pH close to the $\text{p}K_{\text{a}}$ of the $\text{HCO}_3^-/\text{CO}_3^{2-}$ couple (ca. 10.3); this was likely due to its poor transport properties in Nafion.^[13]

In comparison to phosphate and bicarbonate buffers, the overpotentials in NH_4Cl and NH_4HCO_3 were lower at high current densities ($>5 \text{ A m}^{-2}$). The $\text{NH}_4^+/\text{NH}_3$ couple has a $\text{p}K_{\text{a}}$ of about 9.2, which suggests that it should be possible to maintain the local cathode pH in MFCs around this pH value, thus reducing the cathode overpotential in comparison to using no buffer at all, or using phosphate buffer at high current densities. At current densities lower than 5 A m^{-2} , the cathode in PBS performed better than in NH_4Cl and NH_4HCO_3 because of the buffering effect of the lower $\text{p}K_{\text{a}2}$ of the phosphate. However, current densities of up to 25 A m^{-2} were sustained in NH_4^+ solutions without the LSVs showing an inflection resulting from transport limitation. This good result was an effect of the higher diffusion coefficient for NH_4^+ ($D=1.96 \times 10^{-5} \text{ cm}^2 \text{ s}^{-1}$), compared to the other buffers, as it relatively increases the transport rate of NH_4^+ to the cathode surface. Also, using Nafion as the catalyst binder is advantageous for transporting NH_4^+ , because Nafion is efficient in transporting cations.^[13] We have shown in the past that using phosphate or bicarbonate buffer led to better cathode performance if the Nafion binder was replaced with an anionomer,^[11] Nafion is a preferable binder for NH_4^+ buffer.

The results in Figure 1 show that it is possible to decrease the Nernstian concentration overpotential by >150 mV at current densities $>10 \text{ A m}^{-2}$ using NH_4^+ as a buffer at the same concentrations as phosphate. This is an important result, and has especially favorable implications for the treatment of streams containing high levels of NH_4^+ , such as animal waste. However, it has been shown in the past that NH_3 can be lost through air cathodes in MFCs following deprotonation of NH_4^+ .^[14] Thus, any NH_3 that partitions in the gas phase at the cathode should be recovered. Our results here also explain the lower cathodic overpotentials observed in microbial reverse-

electrodialysis cells (MRCs) containing $>1 \text{ M}$ concentrations in the reverse-electrodialysis stack.^[15] It was recently found that even upon removing the stack in such systems, cathode performance significantly improves if the cathode chamber is just fed with a high concentration of NH_4HCO_3 .^[15b] Similar results have been obtained in studies that focus on nitrogen removal in MFCs, and on using NH_4^+ as a proton shuttle between the anode and cathode chambers in dual-chambered MFCs.^[16]

Next, we studied the impact of NH_4^+ transport on cathode performance using different concentrations of NH_4^+ ; the LSVs are shown in Figure 2. This dataset was successfully modeled, as shown in Figure S1 in the Supporting Information, using the parameters listed in Table 1. Ion transport at the electrode-electrolyte interface and within the catalyst layer occurs by

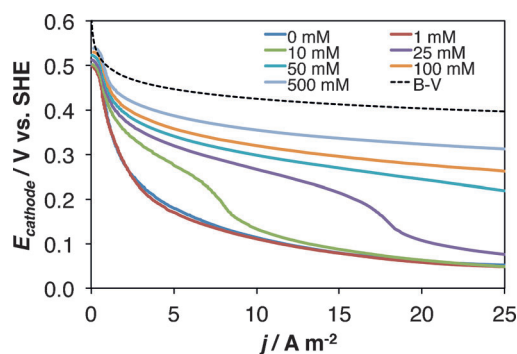


Figure 2. LSVs of a Pt-based gas-diffusion cathode in solutions containing different concentrations (0–500 mM) of NH_4Cl with NaCl (25 mM). The dotted line shows the Butler-Volmer curve on the basis of the j_0 and α values determined from high pH experiments.

two mechanisms: diffusion and migration. The rates of these mechanisms are directly proportional to the concentration of the ion being transported. We hypothesized that cathode performance is limited by buffer transport, and thus could be improved by increasing the concentration of NH_4^+ ; this would allow for faster transport of NH_4^+ to and within the cathode catalyst layer, resulting in lower local cathode pH and lower overpotentials. We tested concentrations of NH_4^+ up to 500 mM, using 25 mM NaCl as background, and the LSVs from these experiments confirm that cathode performance was directly related to NH_4^+ concentration, and thus its transport.

Notably, the inflections in LSVs that we observed earlier with a 50 mM PBS solution, are apparent this time with both 10 and 25 mM solutions of NH_4Cl . A specific modeling result is shown in Figure 3 for the 25 mM NH_4^+ experiment. The model demonstrates that the inflection in the LSV occurs as the dominant species being transported transitions from NH_4^+ to OH^- . This occurs because NH_4^+ transport becomes slower than the production of OH^- , which leads to a pH increase and associated overpotential [Eq. (4)]. At lower buffer concentrations, slower transport of NH_4^+ ions occurs, causing the inflection to occur at a lower current density for 10 mM NH_4Cl versus 25 mM NH_4Cl . At higher concentrations, NH_4^+ transport was not limiting within the range of current densities tested, as it helps maintain the local cathode pH close to the $\text{p}K_{\text{a}}$, as confirmed

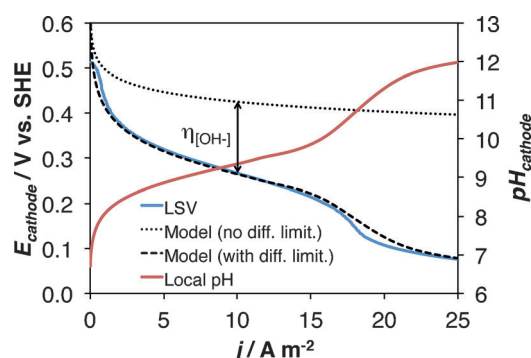


Figure 3. Comparison of LSV of a Pt-based gas-diffusion cathode in NH_4Cl solution (25 mM, with 25 mM NaCl) with model fits from the Butler–Volmer equation without and with diffusion limitation, and the predicted local cathode pH value as a function of current density resulting from NH_4^+ and OH^- diffusion limitation.

by the model fits in Figure S1. Therefore, we saw no inflection points for NH_4Cl concentrations $\geq 50 \text{ mM}$ within the current densities evaluated. In the case of the highest NH_4^+ concentration we tested (i.e. 500 mM), we estimated an $\eta_{[\text{OH}^-]}$ of only about 70 mV at 10 A m^{-2} , and thus the local cathode pH increased only to approximately eight.

An interesting outcome of the model was that the D/L values for NH_4^+ that fit the data were higher than those for OH^- , even though the standard D value for OH^- is roughly 3 times higher ($5.27 \times 10^{-5} \text{ cm}^2 \text{ s}^{-1}$ for OH^- vs. $1.96 \times 10^{-5} \text{ cm}^2 \text{ s}^{-1}$ for NH_4^+).^[17] This suggests that NH_4^+ transport was governed by the diffusion boundary layer, whereas OH^- transport was limited in the catalyst layer. As we mentioned earlier, using Nafion as a binder should allow more efficient transport of cations, and thus NH_4^+ likely diffuses through the catalyst layer a lot faster than OH^- . Because we cannot distinguish individual D/L values for the diffusion boundary layer and the cathode catalyst layer, this shift to limitation in the catalyst layer for OH^- manifests as lower overall D/L values for OH^- .

We also performed similar experiments with different concentrations of phosphate and bicarbonate buffers. The results from these experiments are shown in Figure S2. We observed the same trend with each buffer: an increase in buffer concentration led to a decrease in overpotential and an increase in the current density at which the transition between buffer-governed and OH^- governed transport occurs.

We also performed experiments with different concentrations of NaCl to compare the effect of higher ionic strength versus higher buffering capacity; these results are also shown in Figure S2. This experiment with NaCl clarifies the relative importance of diffusion versus migration in controlling the cathodic overpotentials observed. Although increasing NaCl concentrations improved performance of the cathodes, possibly owing to faster migration transport, the magnitude was significantly lower compared to increasing buffer concentrations.

We performed additional experiments with different concentrations of NaCl (0–500 mM) and NH_4Cl (25 mM) to evaluate the importance of migration in NH_4^+ transport. The results

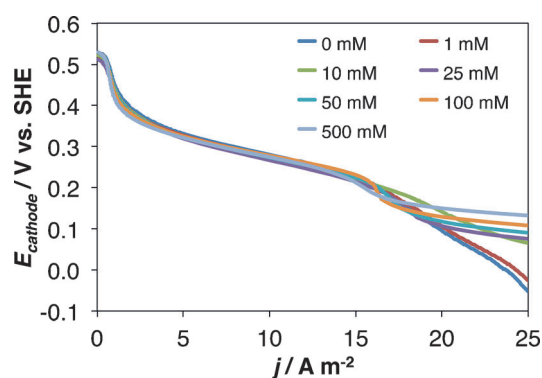


Figure 4. LSVs of a Pt-based gas-diffusion cathode in solutions containing different concentrations (0–500 mM) of NaCl with NH_4Cl (25 mM).

from these experiments are shown in Figure 4. If transport by migration were more important than by diffusion, increasing the concentration of Na^+ would negatively affect cathode performance, as part of the required ion neutrality would be maintained by migration of Na^+ . However, it is apparent that additional Na^+ had no effect on cathode performance up to current densities of about 15 A m^{-2} . Furthermore, no major change was observed in the inflection in the LSVs representing buffer transport limitation. Therefore, migration was less important than diffusion, at least for local transport. This validates our approach of using diffusion as the primary mode of transport in our model described above. It is also consistent with our previous analysis of the anode in MFCs, in which we showed that migration accounted for $< 15\%$ of the local transport to maintain ion neutrality.^[18]

At high current densities ($> 20 \text{ A m}^{-2}$), we observed an effect of Na^+ concentration on cathode performance, with poorer performance at low Na^+ concentrations. This effect was probably due to reaching a limiting current, as a result of the lack of counterions (Na^+) needed to transport OH^- out of the cathode surface.

Finally, we obtained LSVs in NH_4Cl (25 mM, with 25 mM NaCl) with different stirring rates (Figure 5) to investigate the importance of diffusive NH_4^+ transport. If diffusion of NH_4^+ limits cathode performance, decreasing the diffusion boundary

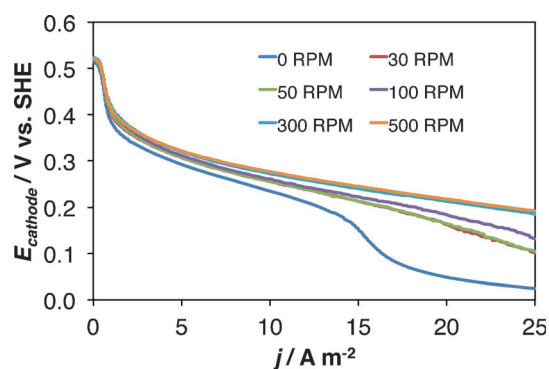


Figure 5. LSVs of a Pt-based gas-diffusion cathode in NH_4Cl and NaCl (25 mM each) at different stirring speeds.

layer by increasing the stirring rate should help achieve higher current densities before the inflection related to transport limitation is seen in LSVs. Even with mild stirring, we observed improved cathode performance at current densities $>10 \text{ A m}^{-2}$. We did not observe an inflection in the LSVs at any of the stirring rates we tested; this confirms that diffusion of NH_4^+ to and within the cathode catalyst layer primarily governed cathode performance.

Modeling results shown in Figure 6 using the experimental results for a stirring speed of 30 RPM confirm that the cathode overpotential depends on the D/L values for NH_4^+ and OH^- (listed in Table 1). At higher stirring speeds, only NH_4^+ transport was important, as the pH did not rise significantly above

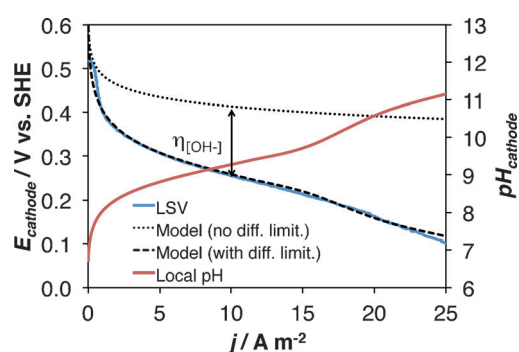


Figure 6. Comparison of the LSV of a Pt-based gas-diffusion cathode in NH_4Cl solution (25 mM, with 25 mM NaCl) at a stirring speed of 30 RPM with model fits from the Butler-Volmer equation without and with diffusion limitation, and the predicted local cathode pH value as a function of current density resulting from NH_4^+ limitation.

the pK_a of NH_4^+ (Figure S3). For 500 RPM, we estimated an $\eta_{[\text{OH}^-]}$ of roughly 200 mV at 20 A m^{-2} , which corresponds to a local cathode pH close to ten. In comparison, without stirring, this was about 400 mV, with a local cathode pH >12 . This represents an improvement in overpotential of approximately 200 mV through improved hydrodynamics. These results suggest that, as MXCs are scaled-up, continuous-flow cathodes could help partially overcome buffer transport limitations by decreasing the diffusion boundary layer. Similar to the experiments with different NH_4^+ concentrations, the D/L value for NH_4^+ that fit the data was higher than that for OH^- . In addition, stirring speed has a stronger impact on the D/L value for NH_4^+ than for OH^- , thus confirming that OH^- transport was more restricted in the catalyst layer.

We performed similar experiments with different stirring speeds with phosphate and bicarbonate buffers, as well as unbuffered NaCl solutions. The results from these experiments are shown in Figure S3. We observed the same trend with each buffer: an increase in stirring speed led to a decrease in overpotential. However, experiments with NaCl showed no effect. This reinforces that diffusion was the primary mechanism of transport on the cathodes for the conditions we tested.

3. Conclusions

We provide the first comprehensive evaluation of cathodic overpotentials and the first model that considers buffer transport. Our results show that cathodic overpotentials in an unbuffered solution are mainly due to concentration overpotential as the pH at the cathode surface rises. The presence of a buffer can alleviate the overpotential from this pH gradient. The effectiveness of the buffer depends on its pK_a and effective diffusivity. Buffers with a pK_a slightly above the operating pH (near neutral) help maintain the cathode local pH close to the bulk pH, thus reducing concentration overpotentials. In this regard, NH_4^+ was expected and confirmed to be the best buffer to reduce concentration overpotentials, owing to its lower pK_a (9.2) and its higher diffusion coefficient, compared to phosphate and bicarbonate. Our experimental results and model provide a framework to characterize cathodic overpotentials in BFCs and other electrochemical cell applications. Through this framework, we can begin to envision potential solutions to minimize cathodic overpotentials.

Experimental Section

We conducted all experiments in gas-diffusion half-cells as described before,^[11] except that 27 mL cells (3 cm \times 3 cm \times 3 cm) were used. We prepared cathodes (9 cm²) as described before, with a Pt loading of 0.5 mg cm^{-2} and a Nafion solution (5%) as the catalyst binder. We obtained LSVs for cathodes in different buffers under quiescent conditions, including individually 50 mM solutions of phosphate buffer (PBS; containing 35 mM Na_2HPO_4 and 15 mM NaH_2PO_4 , pH 7.2), NaHCO_3 (pH 7.9), NH_4Cl (pH 6.5), and NH_4HCO_3 (pH 7.9). We compared these against LSVs obtained in an unbuffered 50 mM solution of NaCl. We obtained all LSVs at 30 °C, with a scan rate of 2 mVs^{-1} , and we performed i - R correction as described before.^[11] We also carried out experiments focused on understanding NH_4^+ transport by using solutions containing different concentrations (0–500 mM) of NH_4Cl with background NaCl (25 mM) and solutions containing different concentrations (0–500 mM) of NaCl with NH_4Cl (25 mM). For solutions containing 25 mM each of NH_4Cl and NaCl, we performed further experiments with agitation provided by magnetic stirring at different speeds.

Acknowledgements

We would like to thank the United States Office of Naval Research (project no. N000141210344) and the SERDP program (project no. ER-2239) for providing the funding for this study.

Keywords: ammonium · buffer · concentration overpotential · neutral pH · oxygen reduction reaction

- [1] R. O'Hayre, S. W. Cha, W. Colella, F. B. Prinz, *Fuel Cell Fundamentals*, Wiley, New York, 2006.
- [2] a) U. A. Paulus, A. Wokaun, G. G. Scherer, T. J. Schmidt, V. Stamenkovic, V. Radmilovic, M. M. Markovic, P. N. Ross, *J. Phys. Chem. B* 2002, 106, 4181–4191; b) S. F. Lu, J. Pan, A. B. Huang, L. Zhuang, J. T. Lu, *Proc. Natl. Acad. Sci. USA* 2008, 105, 20611–20614.
- [3] a) S. Tsujimura, M. Fujita, H. Tatsumi, K. Kano, T. Ikae, *Phys. Chem. Chem. Phys.* 2001, 3, 1331–1335; b) G. C. Gil, I. S. Chang, B. H. Kim, M. Kim, J. K. Jang, H. S. Park, H. J. Kim, *Biosens. Bioelectron.* 2003, 18, 327–334;

- c) P. Clauwaert, P. Aelterman, T. H. Pham, L. D. Schampelaire, M. Carballa, K. Rabaey, W. Verstraete, *Appl. Microbiol. Biotechnol.* **2008**, *79*, 901–913; d) H. Sakai, T. Nakagawa, Y. Tokita, T. Hatazawa, T. Ikeda, S. Tsujimura, K. Kano, *Energy Environ. Sci.* **2009**, *2*, 133–138.
- [4] a) S. C. Barton, J. Gallaway, P. Atanassov, *Chem. Rev.* **2004**, *104*, 4867–4886; b) K. Rabaey, W. Verstraete, *Trends Biotechnol.* **2005**, *7*, 375–381; c) B. E. Logan, B. Hamelers, R. A. Rozendal, U. Schroeder, J. Keller, S. Freguia, P. Aelterman, W. Verstraete, K. Rabaey, *Environ. Sci. Technol.* **2006**, *40*, 5181–5192; d) S. D. Minteer, B. Y. Liaw, M. J. Cooney, *Curr. Opin. Biotechnol.* **2007**, *18*, 228–234; e) B. E. Logan, *Nat. Rev. Microbiol.* **2009**, *7*, 375–381.
- [5] a) G. T. R. Palmore, H. H. Kim, *J. Electroanal. Chem.* **1999**, *464*, 110–117; b) S. C. Barton, H. H. Kim, G. Binyamin, Y. C. Zhang, A. Heller, *J. Am. Chem. Soc.* **2001**, *123*, 5802–5803; c) S. Tsujimura, B. Tatsumi, J. Ogawa, S. Shimizu, K. Kano, T. Ikeda, *J. Electroanal. Chem.* **2001**, *496*, 69–75.
- [6] a) F. Zhao, F. Harnisch, U. Schroder, F. Scholz, P. Bogdanoff, I. Hermann, *Environ. Sci. Technol.* **2006**, *40*, 5193–5199; b) H. Rismani-Yazdi, S. M. Carver, A. D. Christy, I. H. Tuovinen, *J. Power Sources* **2008**, *180*, 683–694.
- [7] a) F. Zhao, F. Harnisch, U. Schroder, F. Scholz, P. Bogdanoff, I. Hermann, *Electrochem. Commun.* **2005**, *7*, 1405–1410; b) S. Cheng, H. Liu, B. E. Logan, *Electrochem. Commun.* **2006**, *8*, 489–494; c) S. Cheng, H. Liu, B. E. Logan, *Environ. Sci. Technol.* **2006**, *40*, 364–369.
- [8] R. A. Rozendal, H. V. M. Hamelers, C. J. N. Buisman, *Environ. Sci. Technol.* **2006**, *40*, 5206–5211.
- [9] a) H. Liu, B. E. Logan, *Environ. Sci. Technol.* **2004**, *38*, 4040–4046; b) H. Liu, S. Cheng, B. E. Logan, *Environ. Sci. Technol.* **2005**, *39*, 658–662; c) H. Liu, S. Cheng, L. Huang, B. E. Logan, *J. Power Sources* **2008**, *179*, 274–279.
- [10] S. Cheng, B. E. Logan, *Bioresour. Technol.* **2011**, *102*, 4468–4473.
- [11] S. C. Papat, D. Ki, B. E. Rittmann, C. I. Torres, *ChemSusChem* **2012**, *5*, 1071–1079.
- [12] a) Y. Fan, H. Hu, H. Liu, *Environ. Sci. Technol.* **2007**, *41*, 8154–8158; b) Y. Feng, X. Wang, B. E. Logan, H. Lee, *Appl. Microbiol. Biotechnol.* **2008**, *78*, 873–880; c) L. Huang, B. E. Logan, *Appl. Microbiol. Biotechnol.* **2008**, *80*, 349–355; d) C. I. Torres, A. K. Marcus, B. E. Rittmann, *Biotechnol. Bioeng.* **2008**, *100*, 872–881.
- [13] A. M. Kiss, T. D. Myles, K. N. Grew, A. A. Peracchio, G. J. Nelson, W. K. S. Chiu, *J. Electrochem. Soc.* **2013**, *160*, F994–F999.
- [14] J. R. Kim, Y. Zuo, J. M. Regan, B. E. Logan, *Biotechnol. Bioeng.* **2008**, *99*, 1120–1127.
- [15] a) R. D. Cusick, Y. Kim, B. E. Logan, *Science* **2012**, *335*, 1474–1477; b) R. D. Cusick, M. C. Hatzell, F. Zhang, B. E. Logan, *Environ. Sci. Technol.* **2013**, *47*, 14518–14524.
- [16] a) R. Cord-Ruwisch, Y. Law, K. Y. Cheng, *Bioresour. Technol.* **2011**, *102*, 9691–9696; b) K. Y. Cheng, A. H. Kaksonen, R. Cord-Ruwisch, *Bioresour. Technol.* **2013**, *143*, 25–31.
- [17] J. R. Welty, C. E. Wicks, R. E. Wilson, G. L. Rorrer, *Fundamentals of Momentum, Heat, and Mass Transfer*, Wiley, New York, **2008**.
- [18] A. K. Marcus, C. I. Torres, B. E. Rittmann, *Electrochim. Acta* **2010**, *55*, 6964–6972.

Received: March 17, 2014

Revised: May 29, 2014

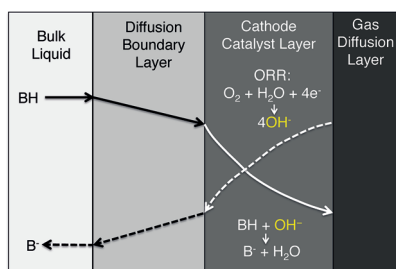
Published online on ■ ■ ■, 2014

ARTICLES

S. C. Popat,* D. Ki, M. N. Young,
B. E. Rittmann, C. I. Torres*



Buffer pK_a and Transport Govern the Concentration Overpotential in Electrochemical Oxygen Reduction at Neutral pH



Chemistry in the buff(er): The importance of buffer in mitigating high local pH on cathodes in biological fuel cells is explored. NH_4^+ is found to be the best out of the tested buffers because of a more relevant pK_a , and also better effective diffusivity. A model, which includes Butler–Volmer kinetics and buffer diffusion, is presented and accurately describes cathode polarization curves. BH = acidic buffer species, B^- = basic buffer species, ORR = oxygen reduction reaction.